Gallium Arsenide. (Proceedings of the 2nd International Symposium, 1968)

GALLIUM ARSENIDE

Proceedings of the Second International Symposium
organized by
Southern Methodist University
and
The Institute of Physics and The Physical Society
in co-operation with
The Avionics Laboratory of the U.S. Air Force

Dallas, Texas, October, 1968

Institute of Physics and Physical Society
Conference Series No. 7

The Second International Gallium Arsenide Symposium was held at Southern Methodist University, Dallas, Texas, on 16–18 October 1968.

Organizing Committee

Dr. H. Strack (Chairman)
Dr. W. Carr
Dr. J. Franks
Dr. J. Lamorte
Col. R. Runnels

Editor

C. I. Pedersen
assisted by E. L. Dellow

SBN 85498 002 4

Published by
THE INSTITUTE OF PHYSICS AND THE PHYSICAL SOCIETY
47 Belgrave Square, London, S.W.1
Editorial Department: 1 Lowther Gardens, Prince Consort Road, London, S.W 7

Printed in Great Britain by
Adlard & Son Ltd, Dorking, Surrey

Contents

Preface

It has been the intent of the sponsors of the 'International Conference on Gallium Arsenide' series to give specialists in the field of research on gallium arsenide devices and materials an opportunity of interchanging ideas and to provide an up-to-date survey of the gallium arsenide technology. Because of the similarity of the technology of gallium arsenide and that of its alloys with other III–V compound materials, the 1968 conference included papers on $Ga_xAl_{1-x}As$, $Ga_xIn_{1-x}As$ and $GaAs_xP_{1-x}$. It is of interest to compare the papers given at the 1966 and 1968 conferences to establish progress made within the last few years, to identify new materials, devices, and technologies, and to visualize trends in the gallium arsenide field.

The papers were divided into four major categories: materials, light emitters, microwave devices, and other devices. Based on the number of papers presented in each category, the interest in the materials area has considerably increased over the past two years, and the work on microwave devices has decreased. This might indicate that researchers improve the material first before expanding a large device effort. The light emitter work, both in the area of spontaneous and stimulated emission, dominates other gallium arsenide device work. In the section on 'Other Devices', the interest has shifted from bipolar and MIS field-effect transistors to Schottky barrier field-effect transistors. A new device, the gallium arsenide photocathode, was not reported on during the last conference.

In the 1966 conference no papers in the materials session dealt with liquid epitaxy, while a whole session was devoted to this subject in 1968. The most remarkable observation is that solution-grown gallium arsenide reached the purity level of vapour-phase material. Materials with a carrier concentration in the low 10^{13} cm^{-3} and with liquid nitrogen mobilities of 13,500 $cm^2\ v^{-1}\ s^{-1}$ have been obtained. One material was not even considered as a material for device fabrication at the time of the last conference. Now, GaAlAs might become an important material for fabrication of light emitters in the visible red wavelength region.

Other material papers discussed advanced research on vapour-phase growth. All aspects of this field such as doping of vapour-phase epitaxial material, the effect of the growth direction on growth rate and doping level, and the growth of high purity, high mobility material were discussed. Reports on bulk gallium arsenide covered subjects such as the properties of dislocation-free material and the behaviour of amphoteric dopants in gallium arsenide.

Most device papers concerned themselves with spontaneous and stimulated light emitters. Progress has been made both in understanding the light emission characteristics and in fabrication of devices with high quantum efficiency. The injection mechanism of diffused junctions has been thoroughly investigated, as well as the phenomena of unconventional light emitters such as filamentary emission in semi-insulating GaAs and two-photon absorption emitters. The laser field has reached a degree of maturity with most papers reporting on special aspects of lasers rather than on device fabrication. This is not the case in the microwave device area, where problems such as the influence of materials properties on microwave diode and Gunn oscillator performance, as well as design calculations for LSA oscillators were discussed.

In the session on 'Other Devices', several papers dealt with various types of gallium arsenide transistors. Though the gallium arsenide transistor was one of the first III–V compound devices and now has a ten-year history, a useful device has not been achieved yet. At the 1966 conference it was reported that bulk states limit the high frequency performance of bipolar devices and surface states limit MIS field-effect transistors. At the 1968 conference some of the problems of the newly developed Schottky barrier field-effect transistor seem to be related to interface states. Transistors developed for the other possible applications for gallium arsenide, the high temperature electronics field, suffer at the present time from high junction leakage currents. The remainder of the

papers dealt with optoelectronic devices such as photodetectors and photocathodes. It is expected that III–V compound optoelectronic devices, including emitters and detectors, will see the strongest expansion in years to come.

The *Proceedings* will have achieved their purpose if the major trends in the gallium arsenide field are reflected and if stimulating ideas are given to researchers planning their work for the following years.

H. STRACK

October 1968

Derivation of the Ga–Al–As ternary phase diagram with applications to liquid phase epitaxy†

M. ILEGEMS and G. L. PEARSON

Stanford Electronics Laboratories; Stanford University, Stanford, California 94305, U.S.A.

Abstract. The ternary liquidus-solidus Ga–Al–As phase diagram has been calculated under the assumptions that the Ga–As and Al–As binary systems are quasi-regular and that the mixed crystals form an ideal solid solution as suggested by the fact that the lattice constants of GaAs and AlAs are nearly identical. Excellent agreement is obtained with experimental liquidus and solidus isotherms obtained in the gallium rich region of the diagram. The liquidus lines were determined at 1000, 900, and 800°C using a weight-loss technique. The solidus composition measurements were made on epitaxial layers of $Ga_xAl_{1-x}As$ grown on ⟨111⟩ GaAs substrates out of gallium-rich melts using a vertical solution regrowth system. The growth temperature was 1000°C and compositions ranging from approximately 20 to 80% AlAs were obtained from melts containing between 0·4 and 4·6% Al.

1. Introduction

Solution grown $Ga_xAl_{1-x}As$ is a promising material for use in a wide variety of applications such as light-emitting diodes, injection lasers, and high voltage p–n junctions. While this mixed crystal compound can be grown from the liquid by essentially the same techniques as those used for GaAs, special problems arise from the addition of a third component to the melt. In particular the composition of the layers is a complex function of melt composition and growth temperature, thus making composition control and homogeneity difficult to achieve even when growing over a limited temperature range. In this paper experimental data obtained for several isotherms in the Ga-rich region of this system will be presented and these will be shown to be consistent with the theoretical analysis presented in section 3. The calculations are then extended to several other liquidus and solidus isotherms and are used to assess the composition variations to be expected during growth in which the growing solid interface is in equilibrium with the liquid phase. The experimental results are in good agreement with these reported recently by Panish and Sumski (1969).

2. Experimental crystal composition and solubility data

A vertical solution regrowth setup similar to that described by Rupprecht (1966) was used in this work. The crucible is alumina and the seed was clamped either between two quartz plates or between two plates of boron-titanium-nitride.

2.1. *Crystal growth*

In a typical growth experiment the crucible was loaded with 5 to 8 g of Ga, 20 to 200 mg of Al depending on the desired crystal composition and the exact amount of GaAs source material required to saturate the melt at the specified growth temperature. At the same time the substrate was mounted in the seed holder and positioned at the top end of the reaction tube. The substrates were slices of ⟨111⟩ oriented GaAs single crystal approximately 5 mm wide, 10 mm long and 0·5 mm thick which had been lapped and chemically polished. The system was heated under a purified stream of hydrogen to the temperature of growth, usually 1000°C, and kept there for a saturation period of 1 hour. Growth was started by

† This work was sponsored by the Advanced Research Projects Agency and the U.S. Army Mobility Equipment Research and Development Center.

lowering the seed holder very slowly into the hot zone of the furnace and dipping the seed into the melt. Cooling rates were usually around 15 to 20°C h^{-1}. It is assumed that under these conditions the growing solid surface is essentially in equilibrium with the melt. Layer thicknesses varying from 250 μm at low Al concentrations to about 50 μm at higher Al concentrations were obtained for a cooling interval of 100°C. The layers were not flat and had to be polished before optical and electrical measurements could be made. Room-temperature carrier concentrations, measured by the Schottky barrier technique, on undoped material were in the low 10^{16} cm^{-3} range. Since only high purity starting materials were used the crucible may have been the main source of contamination.

The crystal composition is determined by the composition of the melt and the temperature of growth. Since the layers are not homogeneous in depth, estimation of composition from optical transmission data is difficult and, at present, electron beam probing appears to be the only practical method.

The experimental composition data versus the Al concentration in the melt are shown in figure 1. The sample with the lowest AlAs concentration was grown by cooling from 1000°C over a 100°C interval, and the composition measured on the substrate side of the

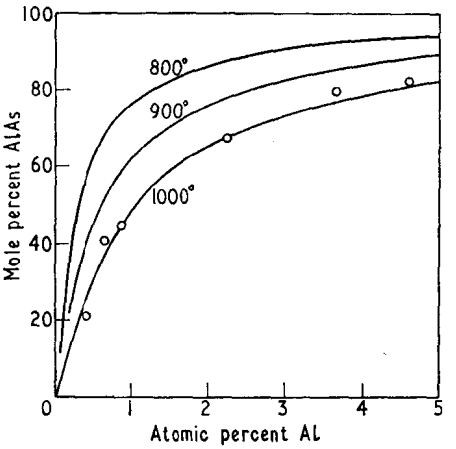

Figure 1. Crystal composition as measured by electron beam probe versus melt composition for samples grown at 1000°C. Solid lines are calculated.

layer after the substrate had been lapped away. All other samples were grown by cooling from 1000°C over a temperature interval less than 20°C, and compositions were measured directly on the growth side of the layer.

The electron beam probing was carried out by the Materials Analysis Company. The Ga and Al concentrations were both measured and the results agreed within the order of five per cent after corrections for absorption, so that the uncertainty in x was estimated at $\pm 5\%$. Samples of high Al content were exposed to air for the shortest possible time and kept in a dry hydrogen stream or under vacuum without apparent decomposition. The material appears to be stable in air up to about 60% AlAs.

2.2. *Liquidus composition measurements*

In order to start crystal growth at the exact equilibrium temperature it was found advantageous to establish the equilibrium condition prior to each run by dipping a piece of polycrystalline GaAs source material in the melt for 20 to 30 minutes. By measuring the weight-loss after dipping and repeating the procedure for a series of different temperatures and compositions the liquidus isotherms were determined experimentally in the Ga-rich region of the diagram. The solubility data obtained at 1000, 900 and 800°C are plotted as

a function of the Al/Ga weight ratio in the melt in figure 2. The melt was kept at the saturation temperature for approximately 30 minutes before dipping and was stirred frequently during dipping by rotating the seed holder.

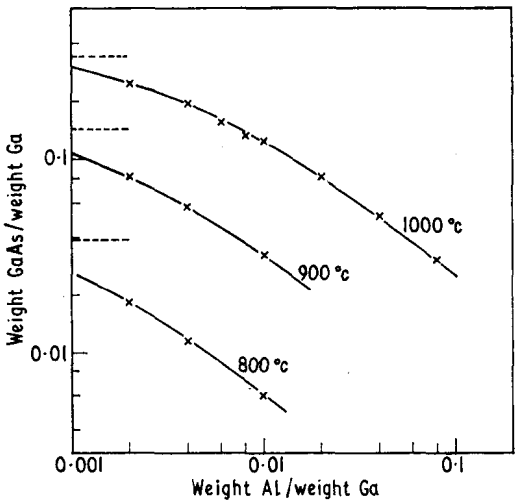

Figure 2. Solubility of GaAs versus Al concentration in the Ga–Al melt at 1000, 900, and 800°c. The dashed lines correspond to the values in pure Ga.

As soon as sufficient GaAs has dissolved in the melt to reach the liquidus composition any further dissolution of GaAs will result in the formation of the mixed $Ga_xAl_{1-x}As$ crystals in equilibrium with the melt at that temperature. The mixed crystals will be formed in the region immediately surrounding the seed and apparently deposit as a thin layer on the seed thereby protecting it from further attack. That a true equilibrium situation was established in this manner was verified by repeating several measurements at longer dipping times (up to 90 minutes at 1000°c) where it was found that the weight loss increased only very slightly as might be expected from temperature fluctuations and evaporation of As from the seed.

3. Interpretation of the data

The experimental results presented above can only be properly understood with reference to the conditions of chemical equilibrium between the mixed crystals and the melts from which they were grown. An analysis of these equilibrium conditions is presented next and shows that the experimental data are consistent with theory. The representation adopted for the three binary systems which form the boundaries of the ternary phase diagram will be discussed first and their deviation from ideality characterized in terms of the interaction energy $\alpha = \Delta G_m^e/N_A N_B = (\Delta H_m - T\Delta S_m^e)/N_A N_B$ in the liquid phase, where ΔG_m^e is the excess free energy of mixing. The equilibrium conditions will then be derived in terms of the chemical potentials μ, making the assumption that GaAs and AlAs form ideal solid solutions as suggested by the fact that their lattice constants are nearly identical.

3.1. *Ga–Al system*

The Ga–Al system was analysed using the method developed by Hiskes and Tiller (1968). Deviations from ideality were found to be fairly small and to have only a limited influence on the phase diagram calculations. In order to keep the activity coefficient relationships consistent with the Gibbs–Duhem equations, a strictly regular representation was adopted for this system and only the first term ($\alpha_{GaAl} = 104$ cal/mole) was kept in the expansion obtained for α.

3.2. *Ga–As system*

The phase equilibria in this system have been analysed by Thurmond (1965) and Arthur (1967). Calculating α from the liquidus data following Vieland (1963), it was found that α was a linear function of temperature so that the binary liquid could be described as quasi-regular. In our calculations this representation was adopted and the expression $\alpha_{GaAs} = -9{\cdot}16T + 5160$ cal/mole was taken from Arthur (1967).

By analysing all III–V compound solutions for which experimental data are given and using published experimental values for the entropies of fusion when available, it was found that the quasi-regular approximation was valid in all cases within the uncertainty in the experimental data. It was observed, moreover, that all α versus T lines had approximately the same slope for a given group V element, indicating the same degree of association in the liquid, while the heat of mixing term decreased regularly as one goes down the column III elements. This similarity in behaviour enables reasonable estimates to be made in section 3.3 for the Al–As system even though few experimental data are available in the literature.

3.3. *Al–As system*

No experimental liquidus data have been reported on this system but from the preceding discussion it seemed reasonable to assume that the Al–As system is quasi-regular with a value for the excess entropy of mixing equal to that of Ga–As. With this assumption the α versus T line will be completely determined if the value of α at one particular temperature is known. This single value of α is derived here from the standard heat of formation of AlAs, $\Delta H_{298} = -27{\cdot}8 \pm 0{\cdot}5$ kcal/mole from Kischio (1964), by calculating the free energy of formation of the compound from the pure liquid components at the melting point. The result is $\Delta G_{AlAs} = -10{\cdot}25 \pm 1{\cdot}8$ kcal/mole at the melting point of 2013°K as reported by Kischio (1964). The derivation was carried out by (1) using the free energy functions for Al and As given by Stull and Sinke (1956), (2) taking the specific heat of liquid As equal to that of solid As at the melting point, (3) adopting the value for the heat of fusion of As selected by Thurmond (1965), and (4) assuming that the specific heat of AlAs is the same as that given for GaP by Thurmond (1965). The rather large error limit in ΔG_{AlAs} arises by assuming that any or all of the estimated specific heats may be in error by 10% over the entire temperature range and includes the 0·5 kcal/mole error in the standard heat of formation.

From $\Delta G_{AlAs}(2013)$ the value $\alpha_{AlAs}(2013) = -9{\cdot}4$ kcal/mole is obtained so that in the quasi-regular approximation the Al–As binary system is described by

$$\alpha_{AlAs} = -9{\cdot}16T + 9040 \text{ cal/mole}.$$

3.4. *Equilibrium conditions between solid and liquid phases*

The activity coefficients and the chemical potentials in the liquid phase can be derived from the α's given in the previous sections. Following Prigogine and Defay (1965), the relation for a three-component system is

$$RT \ln \gamma_{Ga} = \alpha_{GaAs} N_{As}^2 + \alpha_{GaAl} N_{Al}^2 + (\alpha_{GaAs} - \alpha_{AlAs} + \alpha_{GaAl}) N_{As} N_{Al}, \quad (1)$$

where γ_i and N_i designate respectively the activity coefficient and concentration of constituent i in solution. Only the formula for Ga has been given since the other two can be deduced by cyclic permutation of the indices. These equations obey the Gibbs–Duhem relationships and reduce to the appropriate binary form at the boundaries.

The chemical potentials in the liquid phase are given by equations of the form

$$\mu_{Ga}^{l}(T) = \mu_{Ga}^{ol}(T) + RT \ln \gamma_{Ga} N_{Ga}, \quad (2)$$

and in the solid phase by

$$\mu_{GaAs}^{c}(T) = \mu_{GaAs}^{oc}(T) + RT \ln x. \quad (3)$$

Here the superscripts o, l, and c refer to the pure state, the liquid phase and the crystalline phase respectively; x designates the GaAs fraction of the $(GaAs)_x (AlAs)_{1-x}$ mixed crystals which are assumed to form perfect solid solutions. A similar equation applies to AlAs.

The chemical potential of the pure compound which appears in equation (3) can be related to the chemical potentials of its constituents in the liquid phase by the following formula given by Vieland (1963):

$$\mu_{GaAs}{}^{oc}(T)=\mu_{Ga}{}^{sl}(T)+\mu_{As}{}^{sl}(T)-\Delta S_{GaAs}{}^{F}(T_{GaAs}{}^{F}-T) - \Delta C_p\left(T_{GaAs}{}^{F}-T-T\ln\frac{T_{GaAs}{}^{F}}{T}\right), \quad (4)$$

where ΔS^F is the entropy of fusion of the compound, ΔC_p the difference in specific heat between the compound and its supercooled liquid and where the superscript sl refers to the stochiometric liquid. ΔS^F and ΔC_p are assumed independent of temperature.

At equilibrium the chemical potentials of GaAs and AlAs in the mixed crystals must be equal respectively to the sum of the chemical potentials of Ga and As and Al and As in the liquid:

$$\mu_{GaAs}{}^{c}(T)=\mu_{Ga}{}^{l}(T)+\mu_{As}{}^{l}(T) \quad (5a)$$

$$\mu_{AlAs}{}^{c}(T)=\mu_{Al}{}^{l}(T)+\mu_{As}{}^{l}(T). \quad (5b)$$

Substituting equations (2), (3), and (4) into the above equilibrium conditions and solving for x and $1-x$ it is found, neglecting the specific heat terms, that:

$$x=4N_{Ga}N_{As}\frac{\gamma_{Ga}\gamma_{As}}{\gamma_{Ga}{}^{sl}\gamma_{As}{}^{sl}}\exp\left[\Delta S_{GaAs}{}^{F}(T_{GaAs}{}^{F}-T)/RT\right] \quad (6a)$$

and

$$1-x=4N_{Al}N_{As}\frac{\gamma_{Al}\gamma_{As}}{\gamma_{Al}{}^{sl}\gamma_{As}{}^{sl}}\exp\left[\Delta S_{AlAs}{}^{F}(T_{AlAs}{}^{F}-T)/RT\right]. \quad (6b)$$

Elimination of x between these two equations gives the liquidus surface while elimination of T gives the solidus lines. The complete phase diagram can therefore be obtained by calculating the liquidus equilibrium temperature T and the composition x of the mixed crystals in equilibrium with the melt for each set of values of N_{Ga}, N_{Al}, and N_{As}. Unfortunately, the resulting functions have no simple analytical expression and a computer solution must be used.

In the following calculations the value 16·64 cal/mole deg was adopted for the entropy of fusion of GaAs as quoted by Arthur (1967). The entropy of fusion of AlAs has not been reported in the literature but it was found that its value could be estimated from crystal composition measurements. Dividing equation (6*b*) by equation (6*a*) gives the following simple linear relationship between the entropies of fusion of the two compounds and the logarithm of the ratio of the distribution coefficients of Ga and Al:

$$\Delta S_{AlAs}{}^{F}(T_{AlAs}{}^{F}-T)-\Delta S_{GaAs}{}^{F}(T_{GaAs}{}^{F}-T)=RT\ln\left(\frac{1-x}{N_{Al}}\Big/\frac{x}{N_{Ga}}\right)+RT\ln A \quad (7)$$

with

$$RT\ln A=(\alpha_{AlAs}-\alpha_{GaAs})(1/2-N_{As})-\alpha_{GaAl}(N_{Ga}-N_{Al}), \quad (8)$$

as derived from the activity coefficient relationships in the quasi-regular approximation. Substituting for x, N_{Ga}, and N_{Al} from the six experimental composition points in figure 1 and solving for $\Delta S_{AlAs}{}^{F}$ as shown in table 1, values ranging from 21·3 to 23·3 e.u./mole are obtained. An average value of 22·8 e.u./mole was finally adopted for the entropy of fusion of AlAs.

All thermodynamic constants required in solving the phase equilibria equations are now available and tabulated in table 2. Upon substitution in equations (6*a*) and (6*b*) the solidus lines at 1000, 900, and 800°C were calculated and plotted in figure 1. In like manner the

Table 1. ΔS_{AlAs}^{F} **from measured distribution coefficients at 1000°C**

N_{Al} %	N_{Ga} %	x %	$\ln \frac{(1-x)/N_{Al}}{x/N_{Ga}}$	$\ln A$	ΔS_{AlAs}^{F} e.u./mole
0·416	90	79	4·05	0·60	21·3
0·637	90·7	59	4·6	0·60	23·1
0·86	91·4	55	4·46	0·61	22·7
2·26	92·6	32·5	4·45	0·65	22·8
3·65	92·4	20	4·61	0·66	23·3
4·56	92	18	4·52	0·68	22·9

Table 2. Thermodynamic constants used in the calculations

	Ga–As	Al–As	Ga–Al
T^{F}(°K)	1511	2013	—
ΔS^{F}(e.u./mole)	16·64	22·8	—
α(cal/mole)	$-9\cdot16T+5160$	$-9\cdot16T+9040$	104

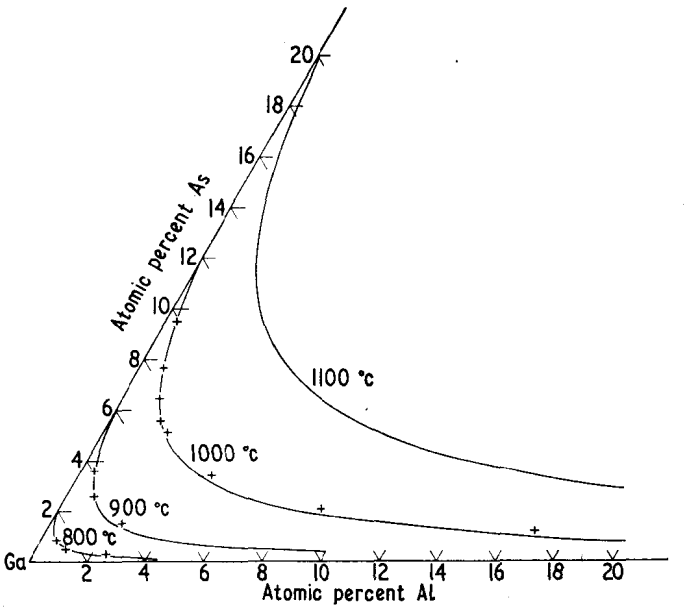

Figure 3. Calculated liquidus lines in the Ga rich region of the ternary diagram. Experimental data points are from figure 2.

liquidus lines in the Ga rich region of the diagram were calculated and plotted in figure 3 for several fixed temperatures. In each case the experimental data points are shown for comparison. The agreement is evident and demonstrates that the composition and solubility measurements are consistent with each other within the framework of the above analysis and that the assumption of ideal solid solutions is essentially correct.

The excellent agreement obtained may at first seem surprising in view of the large uncertainty that goes with the thermodynamic data and the approximations made in this work. However, the manner in which ΔS_{AlAs}^{F} was derived from the composition data makes it an adjustable parameter which compensates for the assumptions in the analysis so that the final liquidus curves are still reliable at least over the region in which composition measurements were made. With this limitation in mind, the liquidus and solidus lines covering the entire phase diagram can be generated from equations (*6a*) and (*6b*).

4. Applications to liquid phase epitaxy

4.1. *Comparison with GaAs solution growth*

Since the Al distribution coefficients are high, only small amounts of Al must be added to the melt to grow crystals throughout the entire composition range from pure GaAs to practically pure AlAs. For this reason the procedures developed for GaAs liquid phase epitaxy in a vertical system can be used with comparable success in the Ga–Al–As system. Due to the very high reactivity of molten Al, an oxide layer may form on the surface of the melt. Difficulties associated with the formation of this crust were minimized by working in a purified hydrogen atmosphere and by starting growth at the equilibrium temperature.

4.2. *Homogeneity of the layers*

A major drawback to the solution growth method arises from the fact that the melt becomes depleted in Al during the growth process so that the composition of the layers varies during the cooling cycle. Depletion of the melt is to some extent offset by the fact that the Al distribution coefficient increases with decreasing temperature as shown in figure 1. Figure 4 shows the combined effect of these two factors upon the composition of the mixed crystals while cooling under equilibrium conditions from 1000 to 800°C.

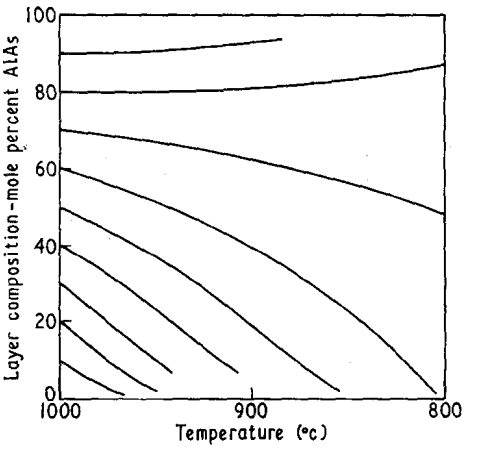

Figure 4. Variation in composition of layers grown during cooling from different initial compositions at 1000°C.

At rates faster than equilibrium the lines shown in figure 4 will tend to be lowered as the region surrounding the substrate becomes more depleted than the remainder of the melt. This indicates that it will be possible to grow homogeneous crystals by this method only in the region around 70 to 80% AlAs since the fall off with temperature is enhanced as the AlAs content decreases.

5. Conclusion

A theoretical analysis of the relationship between melt composition, crystal composition, and growth temperature for crystals grown from a ternary liquid has been presented. The experimental solidus and liquidus data are shown to be consistent with each other in the framework of this analysis and it is concluded that the calculations give a fairly accurate description of the Ga–Al–As system. Finally, although this discussion is in terms of one particular system, the general approach should prove useful when applied to the solution growth of other III–V compound mixed crystals.

References

ARTHUR, J. R., 1967, *J. Phys. Chem. Solids*, **28**, 2257.
HISKES, R., and TILLER, W. A., 1968, *Mater. Sci. Eng.*, **2**, 320.
KISCHIO, W., 1964, *Z. Anorg. Allg. Chemie*, **328**, 187.
PANISH, M. B., and SUMSKI, S., *J. Phys. Chem. Solids*, to be published.
PRIGOGINE, I., and DEFAY, R., 1965, *Chemical Thermodynamics* (London: Longmans), p. 257.
RUPPRECHT, H., 1966, *Proc. Int. Symp. on GaAs*, (London: The Institute of Physics and the Physical Society), p. 57.
STULL, D. R., and SINKE, G. C., 1956, *Thermodynamic Properties of the Elements*, (Washington, D.C.: American Chemical Society), p. 37, 44.
THURMOND, C. D., 1965, *J. Phys. Chem. Solids*, **26**, 785.
VIELAND, L. J., 1963, *Acta Met.*, **11**, 137.

Factors influencing the electrical and physical properties of high quality solution grown GaAs

R. SOLOMON

Fairchild Semiconductor Research and Development Laboratory,
Palo Alto, California 94304 , U.S.A.

Abstract. Growth from gallium solutions is capable of yielding epitaxial GaAs of exceptionally high quality. In this paper, we present experimental results on the effect of several important variables on the electrical and physical properties of these layers.

Boat grown GaAs is used to saturate 7–9's pure Ga in a Pd-purified H_2 atmosphere. Growth temperatures in the range 600 to 900°C and cooling rates from 8 to 300°C h^{-1} have been investigated for several substrate orientations. Results are reported for both a horizontal tilt furnace and a vertical dip furnace.

It is found that oxygen introduces a shallow donor level in solution grown layers, and is probably the principal residual donor in these layers.

Some results are presented for tin doped layers. The mobility at 77°K is compared to theory and provided certain assumptions are made, the fit is reasonably good.

A discussion of the nucleation problem is presented for (100) oriented wafers.

By suitable adjustment of conditions, the technique has consistently yielded layers with net donor concentrations in the range 1×10^{12} to 5×10^{13} cm^{-3}, with LN mobilities in the range 100 000 to 130 000 $cm^2\ v^{-1}\ s^{-1}$.

1. Introduction

Until recently, interest in liquid phase epitaxy (LPE) has centred around heavily doped layers for ohmic contacts and electroluminescent applications. Within the past year or two, however, there has been growing awareness that LPE is also capable of yielding high resistivity, high mobility layers, as has been demonstrated by Kang and Green (1967).

In this paper we will consider some of the factors which influence the electrical and physical properties of high resistivity layers. It will be shown that oxygen contamination is a serious obstacle to achieving high quality results.

2. Experimental technique

In these experiments both a tilt furnace, similar to that used by Nelson (1963), and a vertical dip furnace have been used. In the latter technique a wafer, held in a graphite chuck is dipped into a graphite crucible containing gallium and GaAs. For both furnaces gallium of 7–9's purity is saturated at temperature with boat grown GaAs having a background impurity concentration of $1–3 \times 10^{16}$ cm^{-3}. The furnaces are cooled at programmed rates which vary from 10 to 100°C h^{-1}. The ambient in both furnace arrangements is Pd-purified hydrogen.

The major advantage of the dip furnace is that it is much easier to grow crystals over small temperature intervals, and surfaces tend to be much smoother. On the other hand, the electrical parameters are somewhat inferior to the tilt furnace.

Although the temperature range 600 to 900°C has been explored, most of the work reported here has been performed at lower temperatures, i.e., 600–750°C, than have been previously reported. Our selection of this range stems from our interest in growing relatively thin layers, e.g., from 2 to 15 μ. Although the electrical properties can be relatively independent of temperature over a wide range, low temperature growth does impose special problems with surface smoothness and thickness uniformity.

Most of the effort has been placed on the (100) orientation; however, the (111) B and (110) orientations have also been studied.